ELSEVIER

Ceramics International 30 (2004) 2105–2110

CERAMICS INTERNATIONAL

www.elsevier.com/locate/ceramint

# $MoSi_2$–$Al_2O_3$ electroconductive ceramic composites

Stefan Köbel*, Juliane Plüschke, Ulrich Vogt, Thomas J. Graule

*EMPA Dübendorf, High-Performance Ceramics Laboratory, Überlandstrasse 129, CH-8600 Dübendorf, Switzerland*

Received 5 November 2003; accepted 15 November 2003
Available online 19 March 2004

**Abstract**

$Al_2O_3$–$MoSi_2$ composites with $MoSi_2$ volume fractions between 16 and 40% were fabricated from commercial ceramic $Al_2O_3$ and intermetallic $MoSi_2$ powders by granulation, cold isostatic pressing and vacuum-sintering. The addition of $MoSi_2$ had only a slight influence on the densification of the composites, with sintered densities of 98% for samples with 16 vol.% $MoSi_2$ and 94% for samples with 40 vol.% $MoSi_2$. Composites with $MoSi_2$ contents of 20 vol.% and higher were electroconductive due to the formation of a three-dimensional percolating network of the conductive $MoSi_2$ phase.


*Keywords:* B. Composites; C. Electrical conductivity; D. $Al_2O_3$; D. Silicides

## 1. Introduction

Composites based on highly refractory ceramics in combination with intermetallic compounds show interesting properties, especially at high temperatures. First of all, their good oxidation and corrosion resistance makes them attractive for engineering applications such as in gas turbine engines. Among the numerous combinations of ceramic and intermetallic materials that are thermodynamically stable as a composite, i.e. that do not react with each other during processing or operation, the combination of $Al_2O_3$ and $MoSi_2$ is especially interesting because of the excellent match of their respective coefficients of thermal expansion and thus the absence of residual thermal stresses after sintering and cooling. Thermodynamic modeling suggests that the $Al_2O_3$–$MoSi_2$ system is stable up to 1600 °C, and the high-temperature stability being limited by high vapor pressures of gaseous species like $Al_2O$ and SiO [1,2].

Valuable engineering properties of $MoSi_2$ are its exceptional oxidation and hot corrosion resistance, high melting temperature, high thermal and electrical conductivity and reasonably low density. On the contrary, $MoSi_2$ has a poor low temperature toughness and at elevated temperatures above ∼1250 °C poor strength and creep resistance [1]. $Al_2O_3$ is a refractory oxide, $T_m = 2054$ °C, with reasonable strength and thermal shock resistance. It has a very good corrosion resistance and is an insulator, both at low and elevated temperatures.

Research in the system $Al_2O_3$–$MoSi_2$ is focused on composites with high $MoSi_2$ contents. Those materials are investigated as potential structural materials due to their combination of refractoriness and low density. Alumina is introduced to reinforce the $MoSi_2$ matrix, most often as alumina platelets [3,4] or ceramic fibers [5]. Plasma-spraying was employed to form $MoSi_2$–$Al_2O_3$ lamellar composites [6]. High-temperature thermistors have been developed from $MoSi_2$ and granular $Al_2O_3$ [7]. This composite material consists of $Al_2O_3$ granules with diameters of approximately 150 μm that were coated with $MoSi_2$ and vacuum-sintered at 1650 °C.

$MoSi_2$ has also been employed as conducting phase in $Si_3N_4$–$MoSi_2$ particulate composites [8]. Hot pressing of $Si_3N_4$ with 30 vol.% $MoSi_2$ resulted in a room-temperature conductivity of 3.2 S/cm.

When introducing conductive particles into a nonconductive matrix, like $MoSi_2$ particles into the $Al_2O_3$ ceramic matrix, a certain threshold value for the volume fraction of conductive particles has to be exceeded before the composite becomes electrically conductive. This threshold, commonly called percolation limit, varies with the microstructure in question. The conductive particle shape and their eventual orientation have a particularly strong influence on the percolation limit. While spherical particles in a continuous

* Corresponding author. Tel.: +41-1-823-4199; fax: +41-1-823-4150.
*E-mail address:* stefan.koebel@empa.ch (S. Köbel).

0272-8842/$30.00 
doi:10.1016/j.ceramint.2003.11.015

matrix require 20–30 vol.% to form a percolating network, particles with large aspect ratios, flakes or fibers, require only a few volume percent [9].

A quantitative analysis of the electric conductivity of mixtures of conductive and insulating materials may be done by one of the several models developed that take into account the above mentioned parameters. A comprehensive review of models proposed to explain the electrical conductivity of composites was presented by Lux [10]. For particulate mixtures, several geometrical percolation models were developed to explain the percolation phenomenon. In this work we quantitatively fitted the conductivity data with the GEM equation [11]. It allows calculating the conductivity of a binary composite as a function of composition (volume fractions), the conductivities of the two phases, the percolation threshold, i.e. the critical volume fraction for the phase with higher electric conductivity, and an exponent *t*. Its advantage over the percolation equation is that conductivities for both phases are taken into account, while the percolation equation requires one phase either to be a perfect insulator or a perfect conductor. For these two cases, the GEM equation reduces to a term with the mathematical form of the percolation equation.

In this work we focus on the preparation of composites from mixtures of $Al_2O_3$ ceramic powder with $MoSi_2$ intermetallic powder in the range of 16–40 vol.% and the electric properties of the sintered materials.

## 2. Experimental

Spray drying was used to prepare granules of alumina and molybdenum disilicide with up to 40 vol.% $MoSi_2$. The starting powders (alumina: Alcoa CT3000, molybdenum disilicide: H.C. Starck Grade C) were mixed in water with the addition of an organic binder system (poly(vinyl alcohol), poly(ethylene glycol), surfactant: Zschimmer + Schwartz Dolpapix CE64) and spray-dried (Minor HI-TECH, Niro, DK). Table 1 summarizes the compositions of slurries for spray drying. Green bodies with ~5 mm diameter and 60 mm length were prepared by isostatic pressing at 200 MPa. Sintering was performed in a carbon resistance furnace (FS W 315/400-2200-PC/BL, KCE, D) with samples embedded in coarse-grained fused aluminum oxide powder-bed. The heating rate was 10 °C/min, from room-temperature to the maximum temperature of 1600 °C. During sintering a pressure of ~0.01 atm was maintained.

Table 1
Slurry composition for spray drying

| Substance | Amount (g) | Supplier |
|---|---|---|
| PVA 15000 | 50 | Sigma-Aldrich |
| PEG 300 | 100 | Fluka |
| Dolapix CE64 | 50 | Zschimmer + Schwartz |
| Water, de-ion | 2000 | |

Amounts given for a slurry of 5 kg $Al_2O_3$ or equivalent volume of $Al_2O_3 + MoSi_2$.

A $MoSi_2$ reference sample was processed by isostatic pressing the as-received $MoSi_2$ Grade C powder and sintering identically to the composite samples.

Samples were characterized in respect of their density, microstructure and their electrical properties. Densities were measured by Archimedes' method, immersing liquid for green density measurements was poly(ethylene glycol) ($M$ = 300 g/mol), for sintered samples water was used and relative densities were calculated based on the rule of mixture for $Al_2O_3$ and $MoSi_2$ bulk densities of 4.0 and 6.2 g/cm$^3$, respectively. Microstructural analysis was carried out by scanning electron microscopy (VEGA TS 5136, Tescan, CZ). Coefficients of thermal expansion (CTE) were measured with a dilatometer (Bähr 802, Bähr Thermoanalyse, D) relative to a sapphire reference in air. Electrical properties were determined with a commercial microohm-meter (Resistomat 2318, Burster, D) by 4-probe measurements over 20 mm on as-sintered cylindrical samples of approximately 5 mm diameter. This setup allows to measure samples with conductivities in the range of $10^5$ to $10^{-4}$ S/cm.

## 3. Results and discussion

Granules with mean sizes of 25–40 μm were obtained by spray drying of the aqueous slurries. For all these granules, cold isostatic pressing resulted in cylindrical samples of 5 mm diameter with a green density of ~60% of the theoretical density (%TD).

Sintering of these green bodies at 1600 °C for 90 min resulted in bodies with relative densities of 94%TD for $Al_2O_3$ + 40 vol.% $MoSi_2$ and increase steadily up to 98%TD for $Al_2O_3$ + 16 vol.% $MoSi_2$, as shown in Fig. 1. For the $MoSi_2$ reference sample, the sintered density was 5.93 g/cm$^3$

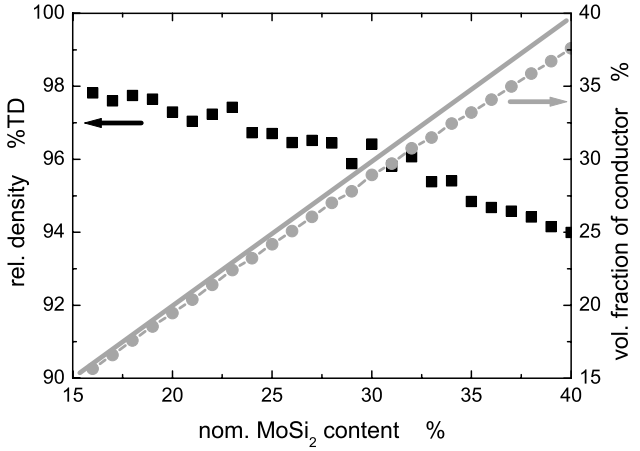


Fig. 1. Sintered densities for $Al_2O_3$–$MoSi_2$ composites vs. nominal $MoSi_2$ content (black squares). Grey circles: volume fraction of $MoSi_2$ vs. nominal $MoSi_2$ content. The solid grey diagonal line indicates the volume fraction of $MoSi_2$ for composites with theoretical density.

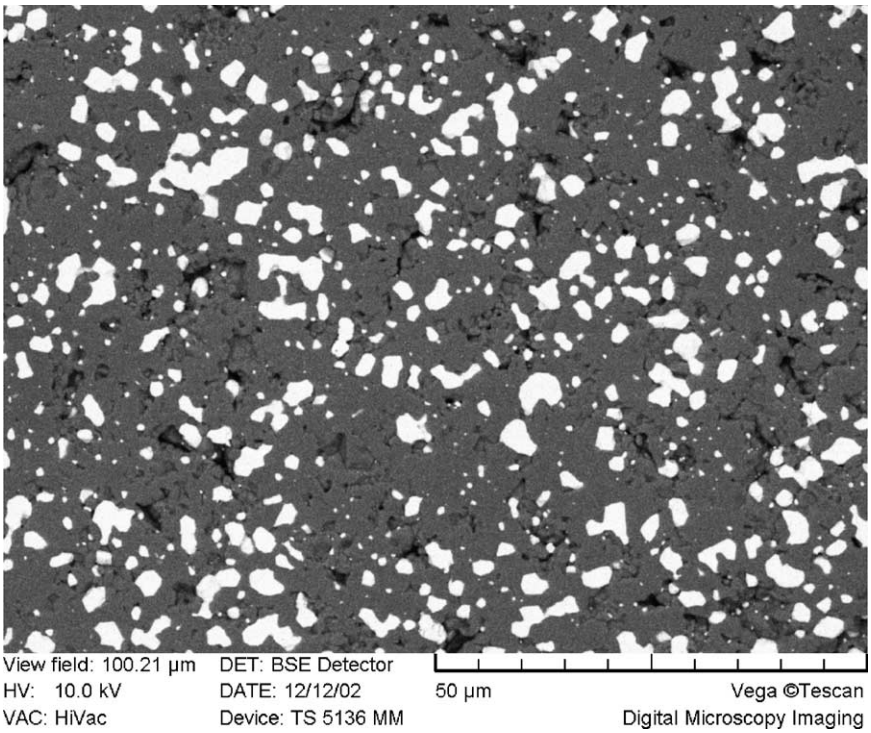


Fig. 2. Secondary electron image of $Al_2O_3 + 20$ vol.% $MoSi_2$. $MoSi_2$ appears white in image. Image width: 100 μm.

or 95.6%TD after applying the same heat treatment. Fig. 1 also shows that the volume fraction of conductor in the sintered samples decreases in the same manner as the fraction of $MoSi_2$ relative to the $Al_2O_3$. For a nominal composition of $Al_2O_3 + 16$ vol.% $MoSi_2$ the volume fraction of $MoSi_2$ is 15.7%, for $Al_2O_3 + 40$ vol.% $MoSi_2$ it is 37.6%. All compositions given in this work refer to the nominal composition, in volume percent; no corrections in regard of the slightly different densities of the sintered samples were made.

Lin et al. [3] prepared composites of $MoSi_2$ with 25 vol.% $Al_2O_3$ platelets. They obtained sintered densities of 89% by sintering the samples in argon at 1700 °C for 2 h. It is evident from our experiments that at least $MoSi_2$ hinders sintering of the $Al_2O_3$ matrix, even though the sintering schedule results in fairly high densities for both, $Al_2O_3$ with small amounts of $MoSi_2$ and for pure $MoSi_2$.

Large voids can be seen from the secondary electron micrographs (Figs. 2 and 3) suggesting that the spray-dried granules partly retain their structure during consolidation by isostatic pressing at 200 MPa. Those cavities cannot be removed by pressure-less sintering and therefore they hinder sintering of the composites to full density.

The X-ray diffraction pattern shown in Fig. 4 reveals that the composites are entirely made of α-$Al_2O_3$ and $MoSi_2$ and no reaction or decomposition of the starting materials occurred.

A major concern for the design of high-temperature composite systems is the difference of thermal expansion of the various phases present. A close match of the coefficients of matrix and dispersed phase is important to minimize the effect of interfacial cracks on the mechanical properties of the composite [12]. Fig. 5 compares the coefficients of thermal expansion of $MoSi_2$ and $Al_2O_3$ with that of the 25 vol.% $MoSi_2$–$Al_2O_3$ composite. At elevated temperatures, the CTE of $MoSi_2$ and $Al_2O_3$ differ by just 4%, hence the influence of the differences in CTE on the mechanical properties is expected to be small if not negligible. The CTE of the 25 vol.% $MoSi_2$ composite is similar to that of the alumina matrix. Tensile stress is therefore induced in the $MoSi_2$ particles. However, we did not find evidence for micro-cracks along the $MoSi_2$–$Al_2O_3$ interfaces nor a degradation of electric properties after repeated heating/cooling cycles. This matches the observation of Lu et al. in alumina platelet and fiber reinforced $MoSi_2$. They addressed matrix cracking in brittle composites by experiment and calculation. Their calculations suggest that cracking in the $MoSi_2$–$Al_2O_3$ composite is most likely to occur between closely spaced fibers or at the edges of platelets. Experiments revealed the absence of cracks for both types of reinforcement, platelets as well as fibers.

Fig. 6 shows the electric conductivities versus $Al_2O_3$ fraction for $Al_2O_3$–$MoSi_2$ composites. Samples with 19 vol.% $MoSi_2$ or less had conductivities below the resolution limit of the setup, approximately $10^{-4}$ S/cm, and thus no conductivity data were obtained. Percolation of the $MoSi_2$ phase starts at ∼20 vol.% and the conductivity for these samples was in the order of $10^{-2}$ S/cm. This is five orders of magnitude lower than that of pure $MoSi_2$. An increase by 1% conducting phase from 20 to 21 vol.% causes the conductivity to rise by a factor of 100. The dependence of the electric con-

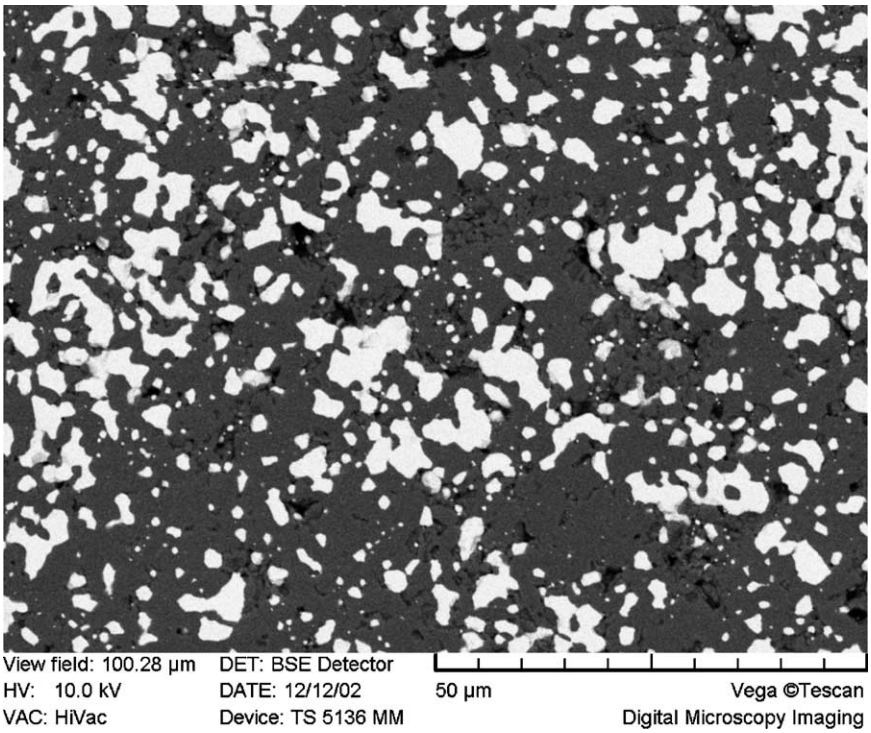


Fig. 3. Secondary electron image of $Al_2O_3 + 40$ vol.% $MoSi_2$. $MoSi_2$ appears white in image. Image width: 100 µm.

ductivity on the composition decreases fast with increasing $MoSi_2$ content, from 25 to 26 vol.% the conductivity rises only by less than a factor of two. Fitting the conductivity data with the GEM or the percolation equation allows estimation of the percolation threshold and the exponent *t*, a phenomenological parameter that characterizes the composite microstructure. A nonlinear least square fitter was used to fit the data in the first place, however, this procedure gives an excellent fit for the high conductivity data but only a reasonable fit for the low conductivity data as can be seen in Fig. 6. A fit with a slightly larger exponent *t*, 2.2 instead of 2.0, seems to represent the experimental data better. All fit parameters are listed in Table 2.

The ordered $MoSi_2$ intermetallic phase shows metallic conductivity with a pronounced positive temperature coefficient of resistance (PTCR). Fig. 7 shows conductivity versus temperature plots for the reference sample of pure $MoSi_2$ and the composites $Al_2O_3 + 40$ vol.% $MoSi_2$ and $Al_2O_3 + 25$ vol.% $MoSi_2$ in the temperature range from 50 to 750 °C. For all samples the TCR is positive over the whole temperature range, however, the lower the $MoSi_2$ content the lower is not only the conductivity but also the TCR. TCRs decrease from $8.2 \times 10^{-3}$ °C$^{-1}$ for $MoSi_2$ to $6.5 \times 10^{-3}$ °C$^{-1}$

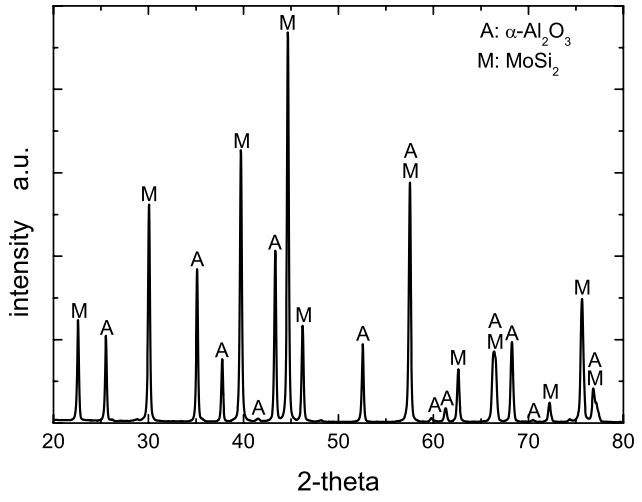


Fig. 4. X-ray diffraction pattern of the $Al_2O_3 + 25$ vol.% $MoSi_2$ composite.

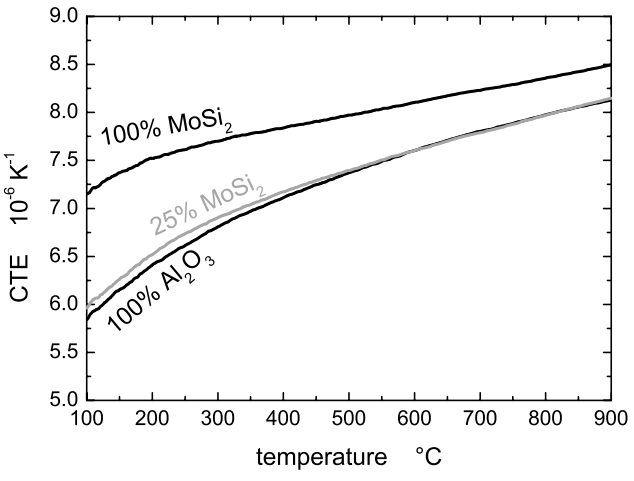


Fig. 5. Coefficient of thermal expansion (CTE) vs. temperature.

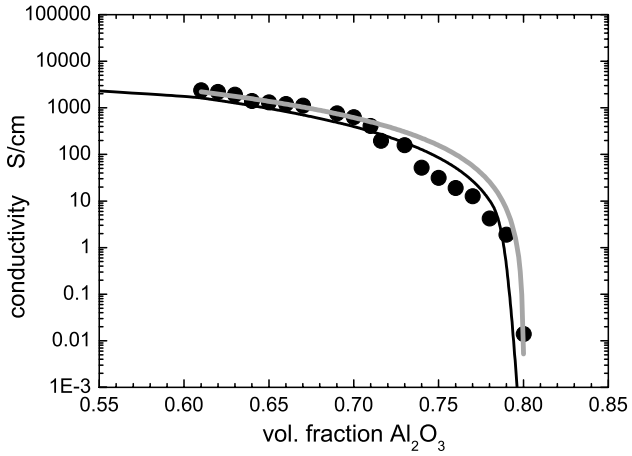


Fig. 6. Conductivity vs. nominal $Al_2O_3$ content. Grey line: fit of the experimental data by applying the percolation equation and a nonlinear least square fitter. Black line: fit "by the eye." Fit parameters are listed in Table 2.

Table 2
Fit-parameters for conductivity vs. alumina fraction data; applied model: GEM-equation

| $MoSi_2$ conductivity (S/cm) | Percolation threshold (vol.% $MoSi_2$) | Exponent | Fit |
|---|---|---|---|
| *38500* | 20.0 ± 1.3 | 1.99 ± 0.09 | NLSF |
| *38500* | *20.0* | 2.2 | "By the eye" |

Numbers set in italic typeface were set constant. NLSF: nonlinear least square fit.

and $4.9 \times 10^{-3}\,^{\circ}C^{-1}$ for composites with 40 and 25 vol.% $MoSi_2$.

## 4. Summary and conclusion

Composites of alumina and molybdenum disilicide were pressure-less sintered to bodies with >94% of the theoretical density. Sintered densities decreased monotonically with increasing amount of $MoSi_2$ from 98%TD for $Al_2O_3$ + 16 vol.% $MoSi_2$ to 94%TD for $Al_2O_3$ + 40 vol.% $MoSi_2$. Processing of the samples by spray drying of an aqueous slurry, isostatic pressing and pressure-less sintering resulted in homogeneous microstructures with finely dispersed $MoSi_2$ particles. However, large voids present in the sintered bodies suggest that the granules were not sufficiently compacted by CIPing at 200 MPa. Thermal expansion coefficients of the composite and the alumina matrix matched perfectly. At elevated temperatures, the CTE of $MoSi_2$ was found to be just 4% higher than that of both, the alumina and the composite. No evidence for micro-cracks along the $MoSi_2$–$Al_2O_3$ boundaries was found. The electrical conductivity increases with $MoSi_2$ content in a manner typical for percolating systems, starting at the percolation limit of approximately 20 vol.%. Composites with more than 20 vol.% $MoSi_2$ show conductivities above the $10^{-2}$ S/cm threshold required for electrical discharge machining (EDM) and may hence be efficiently machined in their sintered state. Electrical conductivities of the samples with different conductor fractions were successfully fitted with the GEM percolation equation.

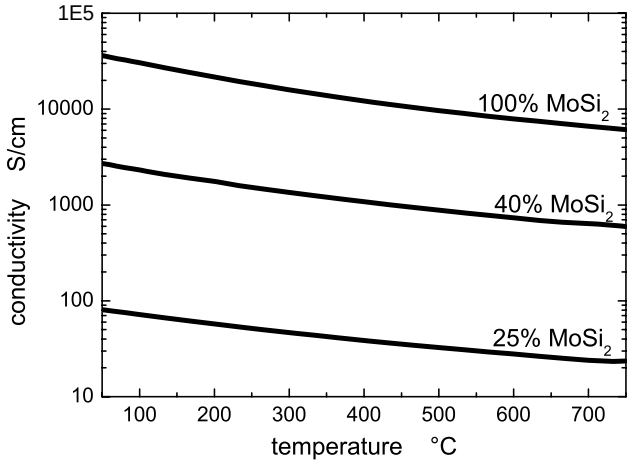


Fig. 7. Conductivity vs. temperature for $MoSi_2$, $Al_2O_3$ + 40 vol.% $MoSi_2$ and $Al_2O_3$ + 25 vol.% $MoSi_2$.

## Acknowledgements

This work has been financially supported by the Swiss Commission for Technology and Innovation, grant no. 5138. The authors are grateful to A. Brönstrup and H.J. Schindler for technical assistance.

## References

[1] A.K. Vasudevan, J.J. Petrovic, A comparative overview of molybdenum disilicide composites, Mater. Sci. Eng. A 155 (1992) 1–17.
[2] H. Wiedemeier, M. Singh, Thermomechanical modeling of interfacial reactions in molybdenum disilicide matrix composites, J. Mater. Sci. 27 (1992) 2974–2978.
[3] G.Y. Lin, V. Costil, Y. Jorand, G. Fantozzi, Experiments on packing and sintering of composite powder mixtures of $MoSi_2 + Al_2O_3$ platelets, Ceram. Int. 25 (1999) 367–373.
[4] T. Watanabe, G.-J. Zhang, X.-M. Yue, Y.-P. Zeng, K. Shobu, N. Bahlawane, Multilayer composites in $Al_2O_3/MoSi_2$ system, Mater. Chem. Phys. 67 (2001) 256–262.
[5] M.J. Maloney, R.J. Hecht, Development of continuous-fiber-reinforced $MoSi_2$-base composites, Mater. Sci. Eng. A A155 (1/2) (1992) 19–31.
[6] D.E. Alman, K.G. Shaw, N.S. Stoloff, K. Rajan, Fabrication, structure and properties of $MoSi_2$-base composites, Mater. Sci. Eng. A155 (1992) 85–93.
[7] H. Yamamoto, S. Sendai, Study on high temperature thermistor made of $MoSi_2$-granular $Al_2O_3$ composite, J. Ceram. Soc. Jpn. Int. Ed. 97 (1989) 770–774.
[8] M.-Y. Kao, Properties of silicon nitride–molybdenum disilicide particulate ceramic composites, J. Am. Ceram. Soc. 76 (11) (1993) 2879–2883.

[9] A. Ishida, H. Matsubara, K. Furukawa, M. Miyayama, H. Yanagida, Computer simulation of percolation structure in composites, J. Ceram. Soc. Jpn. 103 (10) (1995) 996–999.
[10] F. Lux, Models proposed to explain the electrical conductivity of mixtures made of conductive and insulating materials, J. Mater. Sci. 28 (1993) 285–301.
[11] D.S. Machlachlan, M. Blasziewicz, R.E. Newnham, Electrical resistivity of composites, J. Am. Ceram. Soc. 73 (8) (1990) 2187–2203.
[12] T.C. Lu, J. Yang, Z. Suo, A.G. Evans, R. Hecht, R. Mehrabian, Matrix cracking in intermetallic composites caused by thermal-expansion mismatch, Acta Metall. Mater. 39 (8) (1991) 1883–1890.